

Ternary feldspar experiments and thermodynamic models

LINDA T. ELKINS, TIMOTHY L. GROVE

Department of Earth, Atmospheric and Planetary Sciences, Massachusetts Institute of Technology,
Cambridge, Massachusetts 02139, U.S.A.

ABSTRACT

This paper reports the results of 20 experiments in which mixes of two or three feldspars were reacted to produce coexisting plagioclase feldspar (PF) and alkali feldspar (AF). Experiments were carried out over the range 700 to 900 °C and 1 to 3 kbar under water-saturated conditions. The compositions of experimental products were determined using the electron microprobe. Starting materials with similar bulk compositions were prepared using different combinations of two and three minerals, and experiments were designed to produce similar AF and PF minerals in the experimental products from different starting binary and ternary compositions. The coexisting AF and PF compositions produced as products define compositional fields that are elongate parallel to the ternary solvus. In 11 experiments reaction was sufficient to produce fields of coexisting AF and PF, or AF, PF, and melt with a bulk composition close to that of the starting mixture. In six experiments significant reaction occurred in the form of reaction rim overgrowths on seeds of the starting materials, but a tie line connecting AF and PF products lies on the Ab-rich side of the starting bulk composition. In these six experiments some of the An-rich plagioclase starting material was removed from reaction by overgrowth of reaction rims. Three experiments produced AF, PF, and melt from a natural granite starting material. The experiments probably approached stable or metastable exchange equilibrium with respect to Na-K-Ca, but an equilibrium degree of Al-Si order in the rims was most likely not achieved. A thermodynamic model following the approach developed by Ghiorso (1984) and Fuhrman and Lindsley (1988) is applied to these new experimental results. A two-feldspar thermometer is presented in which temperature is constrained by equilibria among all three components—Albite, Orthoclase, and Anorthite—in coexisting ternary feldspars.

INTRODUCTION

Feldspars are a common constituent of crustal igneous rocks, and many igneous and metamorphic rocks contain two feldspars: plagioclase feldspar, consisting primarily of the components anorthite (An, $\text{CaAl}_2\text{Si}_2\text{O}_8$) and albite (Ab, $\text{NaAlSi}_3\text{O}_8$), and alkali feldspar, consisting primarily of orthoclase (Or, KAlSi_3O_8) and albite. A miscibility gap is present in the ternary system, and coexisting alkali and plagioclase feldspar from different geologic settings contain differing proportions of Or, Ab, and An in solid solution. The calibration of changes of the limits of miscibility with temperature and pressure could provide a thermometer and barometer applicable to a wide variety of rocks.

Barth (1951) presented an empirical two-feldspar thermometer, using measurements of the distribution of Ab between naturally occurring plagioclase and alkali feldspars. Temperature estimates were obtained from other indicators of geologic environment. Several more recent feldspar thermometers have also been calibrated using the equilibrium of a single component between coexisting feldspars. The models include those of Stormer (1975),

Powell and Powell (1977), Whitney and Stormer (1977), and Haselton et al. (1983). These models do not include the conditions for equilibrium provided by the other two components, and none of the models consider Al-Si ordering. Thermodynamic models of feldspar equilibria should account for the equilibrium of all three components in coexisting feldspars (Brown and Parsons, 1981) as well as Al-Si distribution. The thermodynamic formulations of feldspar activity-composition relations by Ghiorso (1984), Price (1985), Green and Udansky (1986), and Fuhrman and Lindsley (1988) include constraints from equilibrium among the Ab, An, and Or components in coexisting alkali and plagioclase feldspars.

In this paper we report new experimental data on ternary feldspars. Previous experiments in the ternary system have been carried out by Iiyama (1966), Seck (1971a, 1971b) and Johannes (1979). In these investigations feldspars were synthesized from synthetic gel starting materials, and products were analyzed using powder X-ray techniques on bulk samples or on K-exchanged samples. We used natural and K-exchanged crystalline feldspar starting materials and analyzed the products with an elec-

TABLE 1. Electron microprobe analyses of natural feldspars used as starting materials and bulk compositions of mixes used for the experiments

Feldspar starting materials											
Feldspar*	# of anals	Na ₂ O	K ₂ O	CaO	Al ₂ O ₃	SiO ₂	MgO	FeO	Ab	Or	An
AA	5	11.8(1)	0.16(3)	0.02(1)	19.4(2)	68.6(2)	0.0	0.0	0.990	0.009	0.001
KH	4	8.52(8)	3.44(7)	1.86(2)	21.1(4)	65.5(3)	0.0	0.20(1)	0.721	0.192	0.087
XB	6	2.68(5)	0.07(1)	15.3(1)	32.5(2)	50.2(1)	0.11(1)	0.42(6)	0.240	0.004	0.756
LH	3	10.2(1)	0.22(6)	2.56(2)	21.9(1)	65.3(1)	0.0	0.0	0.867	0.012	0.120
SA	6	7.37(8)	0.05(2)	7.98(4)	26.6(1)	59.2(3)	0.0	0.0	0.624	0.003	0.373
HM											
lamellae	4	11.8(1)	0.05(2)	0.0	19.5(1)	68.5(1)	0.0	0.0	0.997	0.003	0.000
host	5	0.54(2)	15.6(2)	0.0	18.7(1)	65.0(3)	0.0	0.0	0.050	0.950	0.000
HM bulk		3.36	11.7	0.0	18.9	65.9	0.0	0.0	0.304	0.696	0.000
San	6	1.65(4)	14.3(2)	0.0	18.8(1)	65.0(2)	0.0	0.15(4)	0.149	0.851	0.000
KxLH	5	0.28(4)	15.8(2)	1.38(4)	21.2(4)	63.2(7)	0.0	0.0	0.027	0.909	0.064
Bulk compositions used for experiments†											
Mix	Ab:Or:An	Starting minerals	Mix	Ab:Or:An	Starting minerals						
A	73:12:15	HM, XB, AA	A''	67:17:16	KH, XB						
E	69:21:10	HM, XB, LH	G	53:34:13	HM, XB, LH						
I	71:20:9	HM, LH	I'	66:26:8	HM, KH						
J	78:17:5	HM, XB, AA	K	46:31:23	HM, XB, LH						
KL	42:31:27	HM, XB, LH	L	37:31:32	HM, XB, LH						
M	38:37:25	HM, XB, KxLH	O	13:46:41	XB, KxLH						
P	34:34:32	XB, LH, San	Q	31:41:28	XB, SA, San						

Note: Parenthesized units indicate one standard deviation of measurement in terms of least units cited. Therefore, 11.8(1) should be read as 11.8 ± 0.1. Entries of 0.0 mean that element was below detectability limits.

* AA = Amelia albite, Virginia; KH = Kilbourne Hole Anorthoclase, New Mexico, XB = Crystal Bay Bytownite, Minnesota, LH = Lake Harbour, Baffin Island, SA = Sannidal andesine, Norway, HM = Hugo microcline, South Dakota, San = UNT-7002, Eifel sanidine, KxLH = K-exchanged Lake Harbor.

† Letter designations are listed in Table 2 to show bulk composition. Bulk compositions are given as mol% Ab, Or, and An.

tron microprobe equipped with a scanning electron microscope. This analytical method is superior to the X-ray techniques used in previous studies because it quantitatively documents the extent of reaction and compositional variability present in the experimental products.

EXPERIMENTS

Starting materials

Natural feldspars and one K-exchanged feldspar were used as starting materials. Their compositions, as determined by electron microprobe analysis, are in Table 1. Amelia albite from Amelia Courthouse, Virginia, is low albite with highly ordered Al and Si (Thompson et al., 1974; Harlow and Brown, 1980). Kilbourne Hole anorthoclase is a high-temperature ternary feldspar with almost complete Al-Si disorder (Carter, 1970). Crystal Bay bytownite from Crystal Bay, Minnesota, is a labradorite plagioclase consisting of a submicroscopic intergrowth of bytownite and labradorite (McConnell, 1974). Lake Harbor oligoclase, from Baffin Island, is a low temperature plagioclase found in siliceous pods in marble (Grice and Gault, 1983). Sannidal andesine, from Sannidal, Norway, was obtained from the Harvard Mineralogical Museum. Hugo microcline from the Hugo pegmatite, South Dakota, is maximum microcline with highly ordered Al and Si. The sample contains about 24 vol% coarse exsolution lamellae of albite. Compositions of host and lamellae and an estimate of the bulk composition are given in Table 1. UNT-7002 is Eifel sanidine from the Laachersee, Germany (Hovis, 1986). K-exchanged Lake Harbor oligo-

clase was produced by immersing Lake Harbor oligoclase in molten KCl, using the technique described in Orville (1967). A natural granite from the Himalayas (G10) was used as starting material for three experiments. This granite contains microcline, oligoclase, quartz, muscovite, and biotite and has low total Ba (<200 ppm).

Two types of feldspar mixes were prepared and used as starting materials for the experiments. One group of mixes used three feldspars that lay very near or on the Ab-An or Or-Ab binaries. These mixes allowed continuous variation of bulk composition using well-characterized starting materials. When the feldspars in these mixes react, they move away from the binary into the ternary. A second set of mixes consisted of two feldspars. In these mixes one of the starting minerals is a ternary feldspar that lies inside the miscibility gap and that must react toward binary compositions. The bulk compositions of the mixes are in Table 1 and plotted in Figure 1. The feldspars were first ground in an agate mortar under ethanol and then weighed together to make the starting compositions (Table 1). The starting mixes were then ground again to achieve chemical homogeneity. Maximum grain size of the starting materials was 50 μm, and most grains were in the 10 to 20 μm range.

Experimental methods

Approximately 0.1 g of the mixed feldspars were used for each experiment. The crystalline powder was sealed in 19-mm-long Au capsules with 15 μL of distilled H₂O. The capsules were loaded and placed in conventional cold-

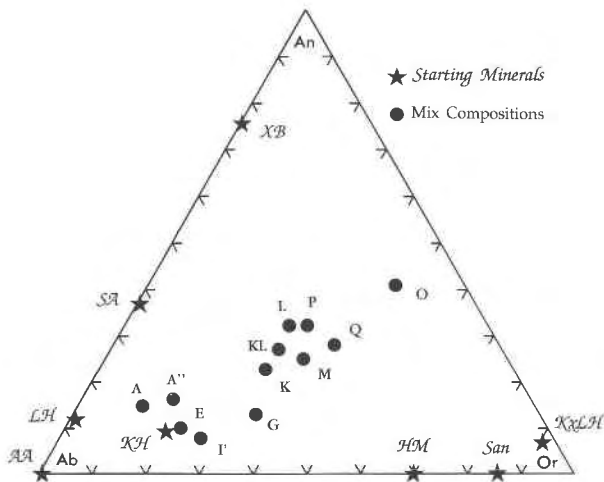


Fig. 1. Compositions of starting mixes used for the ternary feldspar experiments. See Table 1 for compositions and mineral names. Compositions of minerals used as starting materials are shown as stars. Bulk compositions are shown as solid dots. Compositions A, E, G, K, L, M, P and Q consist of mixtures of three starting minerals. Compositions A'', I' and O contain two starting minerals.

seal hydrothermal pressure vessels (Tuttle, 1949). The cold-seal pressure vessels were positioned in the hot spots of horizontal split-tube furnaces so that the temperature gradient over the sample was less than 2 °C. Temperatures were measured with external chromel-alumel thermocouples that were calibrated against a primary thermocouple standardized against the melting point of NaCl. Temperatures were maintained to within ± 5 °C of the stated value. Pressures were measured using a Heise gauge

and maintained to $\pm 2\%$ of the stated value. Experiments were terminated by quenching at pressure in an air jet. The capsules were opened, and the products examined visually. The products were washed, mounted in epoxy, and polished for electron microprobe analysis. Conditions and the duration of the experiments are in Table 2. Only experiments that showed significant reaction are reported. A set of preliminary experiments of varying duration was used to determine minimum experiment times, and these are discussed below.

Analytical techniques

Products were analyzed using the four-spectrometer JEOL model 733 Superprobe at MIT operating at 15 kV and 10 nA. On-line data reduction and the matrix correction procedure of Bence and Albee (1968) with the modifications of Albee and Ray (1970) were employed. Amelia albite, orthoclase glass, DJ35, and cossyrite were used as standards. Amelia albite, Or glass, Lake County labradorite, and synthetic crystalline anorthite were analyzed as secondary working standards to check the primary standardization. Counting times were optimized to provide the lowest possible counting-statistic errors, while minimizing electron beam damage to the samples. We counted Na for 20 seconds as the first element in each analysis. This counting time produced acceptable counting-statistic errors and resulted in no measurable loss in Na X-ray intensity during analysis. Estimates of analytical uncertainties based on counting statistics are on the order of 1 to 2% of the amount present (one standard deviation, 1σ) for major elements present in abundance of 20 wt% or more. Errors estimated from counting statistics for CaO in the alkali feldspar were 8 to 12% of the amount present (1σ). Errors for K₂O in the plagioclase

TABLE 2. Conditions, products and starting materials for ternary feldspar experiments

Run	Duration (days)	T °C	P kbar	Starting* materials	Run products†
L3	18	890	1	HM, XB, LH	AF, PF, Gl, Fl
KL1	17	890	1	HM, XB, LH	AF, PF, Gl, Fl
M1	18	880	1	HM, XB, KxLH	AF, PF, Gl, Fl
O1	17	890	1	KxLH, XB	AF, PF, Gl, Wo, Le, Fl
P2	14	900	1	San, LH, XB	AF, PF, Gl, Fl
G4	27	800	1	HM, XB, LH	AF, PF, Fl
K1	14	800	2	HM, XB, LH	AF, PF, Gl, Fl
L1	14	800	2	HM, XB, LH	AF, PF, Gl, Fl
G3	31	800	2	HM, XB, LH	AF, PF, Gl, Fl
P1	14	800	2	San, LH, XB	AF, PF, Fl
Q1	14	800	2	San, SA, XB	AF, PF, Fl
G2	115	700	2	HM, XB, LH	AF, PF, Fl
E2	115	700	2	HM, XB, LH	AF, PF, Fl
I'1	119	700	2	HM, KH	AF, PF, Fl
A''1	119	700	2	KH, XB	AF, PF, Fl
G10-2	61	700	2	G10	AF, PF, Gl, Fl
G5	102	700	3	HM, XB, LH	AF, PF, Fl
A4	102	700	3	HM, XB, LH	AF, PF, Fl
G10-7	20	675	2	G10	AF, PF, Gl, Fl
G10-9	21	650	3	G10	AF, PF, Gl, Fl
I1	189	600	2	HM, LH	no reaction
J1	189	600	2	HM, XB, AA	no reaction

* Compositions of natural feldspar starting materials are listed in Table 1. G10 is a two-mica granite.

† Abbreviations used for run products: AF = alkali feldspar, PF = plagioclase feldspar, Fl = H₂O-rich fluid, Gl = glass, Wo = wollastonite, Le = leucite.

were 3 to 4% (1σ) of the amount present. X-ray intensities from both Ca and K were counted for 40 seconds. The errors are, in general, smaller than the compositional variability measured in the reaction overgrowths in a single experiment. Minimum detectability limits for Na_2O , MgO , CaO , FeO and K_2O in wt% are, respectively, 0.03, 0.02, 0.02, 0.05 and 0.03.

Backscattered-electron scanning electron microscope (BSE SEM) imaging was used to examine all products of experiments. In BSE SEM imaging the gray levels correspond to differences in average atomic number and thus provide compositional information (Fig. 2). Therefore, BSE SEM imaging was used to evaluate mineral zoning and to distinguish unreacted cores from rims of mineral growth. The rims on product feldspars were identified by BSE SEM imaging and analyzed. Sufficient analytical data were obtained on the rims to determine the compositional variations and the extent of reaction. This compositional variation is represented in Table 3 as averages and 1σ standard deviations. These averages are not intended to represent the best approximation of the equilibrium reaction rim. The averages and standard deviations provide a representation of the compositional variability in the products. For experiments that have reacted extensively, we assume that the equilibrium composition lies within the range of rim compositions analyzed. Furthermore, the compositional variation in the products is not a simple relation of the position of the analysis with respect to the core and rim. In experiments that contain fluid, unreacted cores are surrounded by rims of mineral overgrowth. In experiments that contain melt, some unreacted grains are surrounded by overgrowth rims, and some An-rich and Ab-rich plagioclase can be seen as skeletal relicts in the process of dissolving in the melt.

For many experiments the reaction products are observed to spread along the limbs of the ternary solvus. One explanation for the compositional variability found in the AF and PF products is that the bulk composition of the experiment is changing slowly with time as the relict minerals dissolve. The feldspars that grow from the melt or vapor then change with time in response to the change in bulk composition. Presumably with sufficient time this compositional variability along the miscibility gap would diminish, and a single composition of AF and PF would result. However, the driving force for reaction is small, and experiments of extreme duration would be required to produce completely homogeneous products.

Attainment of equilibrium

Experiments that approach the same final state from different starting conditions demonstrate an approach to metastable or stable equilibrium. To show that our experiments had approached exchange equilibrium for Ca, Na, and K, we used several combinations of starting minerals and allowed the reaction products to grow from different initial compositions. Of the many possible reaction paths, we considered the following three.

Type 1. Both Seck (1971a) and Johannes (1979) at-

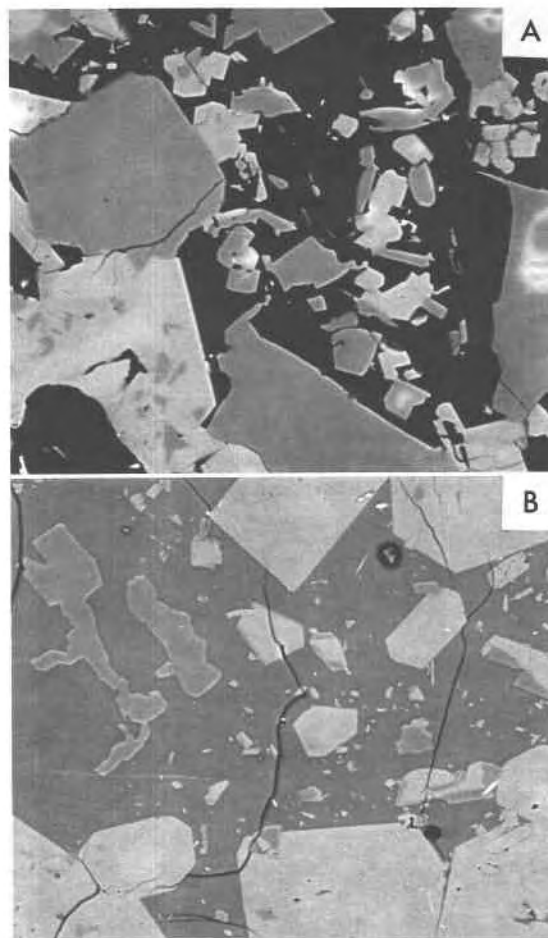


Fig. 2. BSE SEM images of experimental products. (A) Experiment E2, 700 °C, 2 kbar. Dark material surrounding light gray AF and dark gray PF is epoxy. AF crystals contain unhomogenized albite exsolution lamellae. Lighter homogeneous regions in AF are unreacted. Plagioclase is zoned, but zoning is not visible. (B) Experiment G3, 800 °C, 2 kbar. Light gray alkali (AF) and dark gray plagioclase feldspar (PF) are surrounded by melt. AF crystals have unreacted cores and euhedral overgrowth rims. Irregularly shaped, relict PF crystals are dissolving in melt. Small, euhedral PF crystals are growing from melt. Vertical bars at lower left are 10 μm .

tempted to show an approach to similar end-product compositions from different starting materials. Seck and Johannes used two similar bulk compositions. One contained Or-rich AF and Ab-rich PF pairs, and the other contained Ab-rich AF and Ab-poor PF pairs. Under the same experimental conditions, these two compositions then converge to two identical AF and PF pairs. These experiments determine the equilibrium Ca-Na exchange in plagioclase and K-Na exchange in alkali feldspar.

Type 2. For a ternary system with a miscibility gap, one must devise experiments that converge on the equilibrium content of Or component in plagioclase and An component in alkali feldspar. For this approach two types

TABLE 3. Electron microprobe analyses of feldspar products

Experiment	Fsp	# of anals	Na ₂ O	K ₂ O	CaO	Al ₂ O ₃	SiO ₂	MgO	FeO	Ab	Or	An
L3	PF	21	2.70(11)	0.71(20)	14.6(4)	31.4(4)	56.3(6)	0.05(2)	0.31(9)	0.240(10)	0.041(12)	0.719(20)
	AF	15	2.02(4)*	13.4(1)	0.51(8)	19.1(2)	65.0(6)	0.03(1)	0.11(2)	0.182(4)	0.793(7)	0.026(4)
KL1	PF	17	7.36(19)	1.42(13)	5.92(22)	24.8(3)	60.5(4)	0.0	0.07(4)	0.637(17)	0.081(8)	0.283(11)
	AF	21	4.81(28)	9.36(39)	0.75(22)	19.6(3)	65.5(4)	0.0	0.07(5)	0.422(25)	0.541(22)	0.036(10)
M1	PF	36	6.08(23)	1.13(18)	8.06(49)	26.7(5)	57.8(6)	0.0	0.08(2)	0.539(20)	0.066(11)	0.395(24)
	AF	21	3.13(16)	11.5(4)	0.59(10)	19.4(3)	65.4(5)	0.0	0.05(5)	0.283(14)	0.688(23)	0.029(5)
O1	PF	4	1.22(7)	0.30(9)	17.4(4)	33.5(6)	46.2(2)	0.0	0.31(17)	0.111(6)	0.018(6)	0.872(22)
	AF	16	1.15(7)	14.8(2)	0.39(8)	18.8(2)	64.6(4)	0.0	0.09(3)	0.103(6)	0.877(12)	0.019(4)
P2	PF	10	2.76(10)	0.79(17)	14.5(3)	31.1(3)	50.3(4)	0.06(2)	0.54(5)	0.245(9)	0.046(10)	0.709(15)
	AF	5	1.71(8)	12.9(2)	0.66(33)	19.2(1)	61.8(8)	0.03(1)	0.51(31)	0.162(8)	0.804(16)	0.035(18)
G4	PF	35	8.60(27)	2.47(49)	2.75(33)	21.6(3)	65.1(7)	0.0	0.18(5)	0.732(23)	0.138(28)	0.130(15)
	AF	33	5.67(38)	7.96(58)	0.81(22)	19.6(3)	66.1(8)	0.0	0.11(4)	0.499(33)	0.462(33)	0.272(11)
K1	PF	10	7.32(4)	1.52(4)	5.49(8)	24.7(1)	60.6(1)	0.0	0.05(5)	0.645(4)	0.087(2)	0.267(4)
	AF	12	2.87(3)	12.6(1)	0.36(2)	19.2(1)	65.1(1)	0.0	0.05(5)	0.253(3)	0.729(2)	0.018(1)
L1	PF	12	6.78(5)	1.13(3)	6.94(9)	25.9(1)	59.1(2)	0.0	0.06(3)	0.596(4)	0.066(2)	0.338(4)
	AF	15	2.51(3)	12.8(1)	0.35(2)	19.2(1)	65.0(1)	0.0	0.0	0.225(3)	0.757(4)	0.017(1)
G3	PF	11	6.97(3)	1.44(5)	6.91(9)	25.7(1)	60.4(1)	0.0	0.05(5)	0.594(2)	0.081(3)	0.325(4)
	AF	10	2.63(2)	12.7(1)	0.45(3)	19.5(1)	65.9(1)	0.0	0.05(5)	0.234(2)	0.744(6)	0.022(1)
P1	PF	13	7.45(23)	1.18(12)	6.45(45)	25.0(5)	60.6(7)	0.04(1)	0.0	0.632(20)	0.066(7)	0.302(21)
	AF	11	2.87(13)	12.4(2)	0.37(14)	19.2(2)	65.3(9)	0.03(1)	0.06(4)	0.255(11)	0.727(13)	0.018(7)
Q1	PF	7	6.84(13)	1.09(11)	7.68(32)	26.3(3)	59.0(4)	0.03(1)	0.05(5)	0.580(11)	0.061(6)	0.360(15)
	AF	6	2.30(6)	13.3(1)	0.29(2)	19.3(2)	64.9(6)	0.03(1)	0.06(2)	0.206(5)	0.780(8)	0.014(1)
G2	PF	7	8.44(4)	1.01(3)	4.38(7)	23.1(1)	63.4(2)	0.0	0.0	0.732(3)	0.058(2)	0.210(3)
	AF	8	3.02(2)	12.1(1)	0.17(2)	18.6(1)	64.9(2)	0.0	0.0	0.273(2)	0.719(5)	0.009(1)
E2	PF	8	9.18(5)	1.15(3)	3.25(8)	22.1(1)	64.9(4)	0.0	0.07(2)	0.782(5)	0.064(2)	0.153(4)
	AF	13	3.73(3)	11.3(1)	0.18(1)	18.9(1)	66.0(2)	0.0	0.05(5)	0.331(3)	0.660(3)	0.009(1)
l'1	PF	11	8.44(6)	3.78(4)	0.97(2)	20.8(1)	66.1(2)	0.0	0.15(3)	0.736(5)	0.217(2)	0.046(1)
	AF	32	4.31(7)	10.4(1)	0.18(1)	19.2(1)	66.0(1)	0.0	0.0	0.382(6)	0.609(6)	0.009(1)
A'1	PF	8	9.46(4)	1.51(8)	2.55(7)	21.5(1)	65.6(3)	0.0	0.20(3)	0.797(3)	0.084(4)	0.119(3)
	AF	8	4.37(5)	10.1(1)	0.31(2)	19.1(1)	65.6(3)	0.0	0.15(3)	0.392(4)	0.593(7)	0.016(1)
G10-2	PF	10	8.42(10)	1.38(21)	4.23(21)	23.2(3)	63.8(5)	0.0	0.09(3)	0.722(9)	0.078(12)	0.200(10)
	AF	10	2.58(8)	12.5(3)	0.17(2)	18.9(2)	65.5(4)	0.04(1)	0.11(4)	0.236(7)	0.755(19)	0.009(1)
G5	PF	11	9.28(5)	1.19(4)	2.78(4)	21.7(1)	64.9(1)	0.0	0.0	0.801(4)	0.068(2)	0.131(2)
	AF	6	3.54(3)	10.9(1)	0.20(1)	18.9(1)	65.3(2)	0.0	0.0	0.327(2)	0.663(3)	0.010(1)
A4	PF	12	9.07(5)	1.21(3)	3.18(5)	22.1(1)	64.9(2)	0.0	0.14(2)	0.780(4)	0.068(2)	0.152(3)
	AF	7	3.57(4)	11.3(1)	0.25(2)	18.8(1)	66.4(3)	0.0	0.12(2)	0.320(3)	0.667(6)	0.013(1)
G10-7	PF	8	8.26(24)	1.09(21)	4.23(25)	23.1(3)	63.5(5)	0.0	0.0	0.730(21)	0.063(12)	0.207(12)
	AF	10	2.48(8)	12.7(5)	0.14(6)	18.7(4)	66.0(5)	0.0	0.0	0.228(7)	0.765(27)	0.007(3)
G10-9	PF	10	8.69(25)	1.03(10)	3.41(25)	22.3(4)	64.7(8)	0.0	0.06(4)	0.772(22)	0.060(6)	0.167(12)
	AF	12	2.54(13)	12.7(3)	0.10(2)	18.6(2)	65.9(2)	0.0	0.11(4)	0.232(12)	0.763(16)	0.005(1)

Note: Averages represent compositional variation in coexisting AF and PF. Parenthesized units indicate one standard deviation of measurement in terms of least units cited. Therefore, 2.02(4) should be read 2.02 ± 0.04 . An entry of 0.0 indicates that the element was below detectability limits.

of experiments are required. One begins with a ternary composition. The ternary feldspar reacts from within the miscibility gap to coexisting PF and AF feldspar. The second starts with pairs of feldspars from the Ab-An and Or-Ab binary joins, and these react and move into the ternary. The combination of these two types of experiments converge on, and define, the ternary miscibility gap.

Type 3. Experiments are devised to determine the effect of Al-Si distributions among the tetrahedrally coordinated sites on the alkali exchange equilibrium. These experiments should start with feldspars whose Al-Si site occupancy is known. The experiments are conducted using assemblages having different degrees of Al-Si order to test for an effect of Al-Si order on Ca-Na-K exchange. As part of this experiment the Al-Si order of the reacted products must be determined.

We attempted to carry out type 1 and type 2 experiments. For type 1, the three minerals used as starting material were chosen so that we could design experiments that approach similar end-product compositions from dif-

ferent combinations of starting materials. If the product AF and PF, or AF, PF, and melt have a bulk composition that is similar to that of the starting composition, then metastable or stable equilibrium has been approached. The experiments that started with ternary feldspar were our attempt at type 2. Since it is difficult to obtain well-characterized ternary feldspars, we added a binary feldspar to make the mixes similar in bulk composition to that of the type 1 mixes.

Experimental results

In planning these experiments we anticipated that reaction rates would be slow and that reaction overgrowths would occur. Orville (1972) carried out exchange experiments between Ab-An plagioclase and Na-Ca chloride fluid and suggested that the reactions by which plagioclase changed composition occur at different rates in different directions. The rate of the reaction that results in the breakdown of An ($\text{CaAl}_2\text{Si}_2\text{O}_8 + 2\text{Na}^+ + 4\text{SiO}_2 = 2\text{NaAlSi}_3\text{O}_8 + \text{Ca}^{2+}$) to produce Ab is very slow. The reaction rate for the SiO_2 -producing direction is much

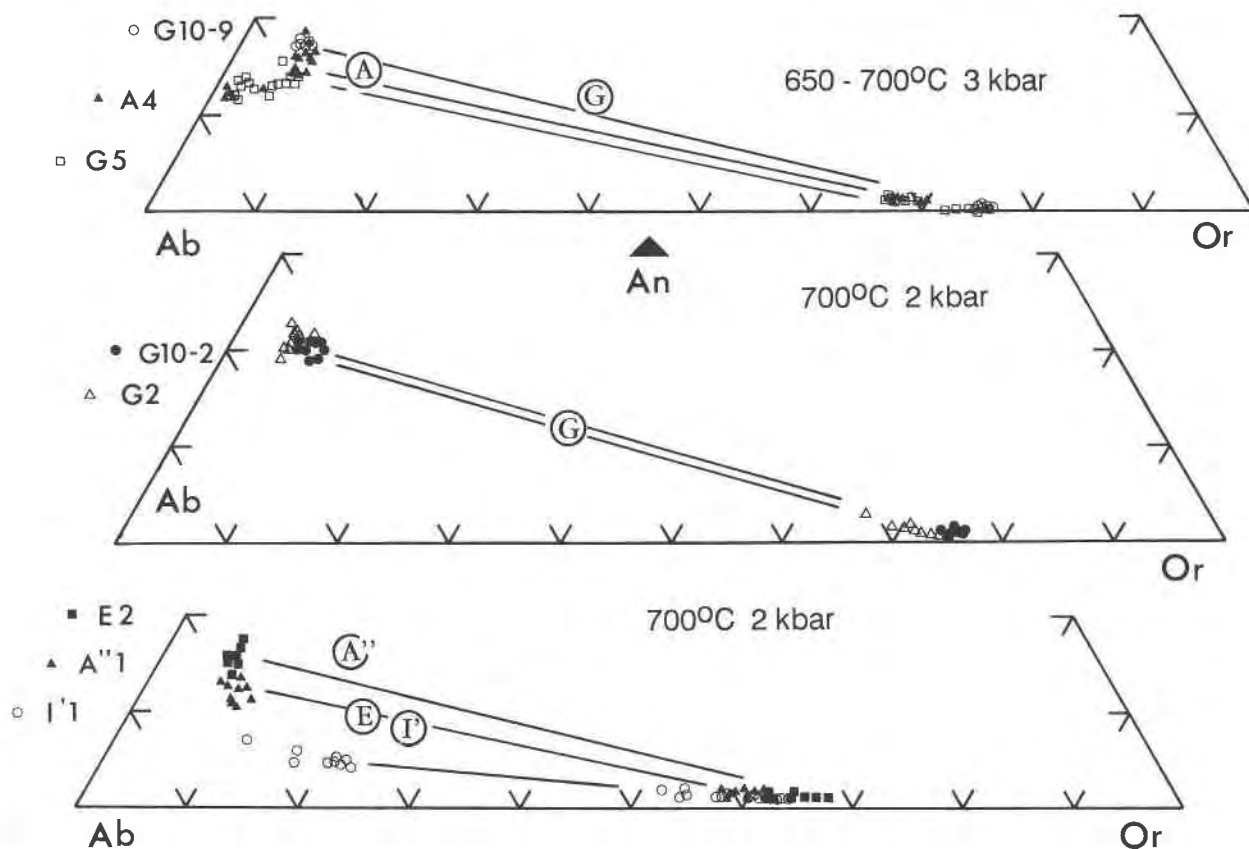


Fig. 3. Compositional variations in AF and PF produced in 2- and 3-kbar experiments over the temperature range 650–700 °C. See Tables 1 and 3 for product compositions and starting materials. Bulk compositions of experiments are indicated by open circles enclosing letters.

faster. Since our starting materials contained both An-rich and Ab-rich plagioclase, experiment times had to be long enough to allow reaction of both. The experiment times of Seck (1971a, 1971b) and Johannes (1979) provided a guide for designing our experiments. Seck used gels as starting materials and claimed that his experiment times were sufficient to grow homogeneous crystalline feldspars. Seck tested times necessary to achieve exchange equilibrium between coexisting crystalline alkali and plagioclase feldspars and found 45 days to be sufficient. Based on this result Seck reacted his gel starting materials for 45 days or less. Seck's experiments at 825 °C and 1 kbar were around 12 days, and those at 650 °C and 1 kbar were around 30 days.

Johannes (1979) used synthetic crystalline starting materials and conducted longer experiments. He questioned the claim that the duration of Seck's experiments was sufficient to produce equilibrium. Johannes also carried out a series of experiments that were conducted from 1 to 45 days and found that experiment times of 40 to 45 days at 800 °C, 1 kbar allowed an approach to metastable or stable exchange equilibrium. He found that 45-day experiments at 650 °C did not produce significant reaction.

Experiments at 700 °C, 2 kbar. As an initial step we determined the minimum experiment times necessary to produce a product assemblage that had the same bulk composition as the starting mix of the natural three-crystal feldspar starting materials. At 700 °C, and 2 kbar, experiments of 46 days (not reported in Table 2) were only beginning to grow reaction rims. Experiments of 98 days (not reported in Table 2) grew reaction rims, but the rim compositions did not cluster tightly at ternary AF and PF compositions. Experiments of 115 days produced rim overgrowth compositions of ternary plagioclase and alkali feldspar that clustered tightly and that lay on a tie line that passed through the starting-mix bulk composition. Figure 3 shows this result for experiment G2, and Figure 4 shows the reactant minerals (HM + LH + XB) and the reaction paths followed to produce ternary AF and PF for G2.

At 700 °C, 2 kbar we attempted both type 1 and two experimental reversals of type 2. Compositions E and G used binary plagioclase and alkali feldspar. Compositions A'' and I' were prepared using a ternary and a binary feldspar (Fig. 4). Experiments E2 and G2 were type 1. Both experiments showed extensive reaction, and a tie line connecting the reactant AF and PF fields passes

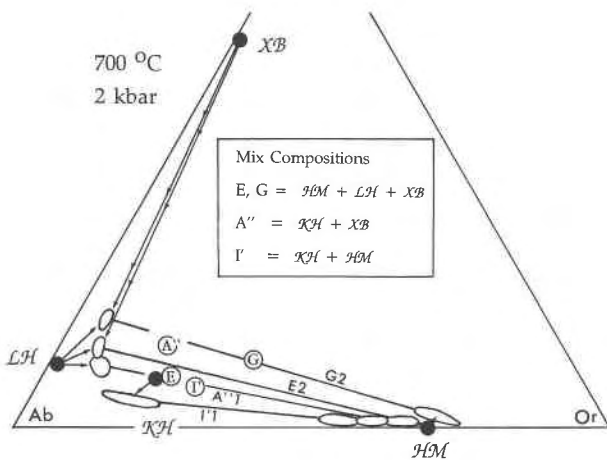


Fig. 4. Products, starting minerals and bulk compositions for selected experiments at 700 °C, 2 kbar. Solid dots and script initials show starting minerals. Bulk compositions are shown by circles enclosing letters. Product compositions lie within the elliptical areas, and AF and PF fields from each experiment are connected by a tie line showing experiment number. Arrows point from starting mineral compositions to reactant products.

through the bulk composition. Experiments A'1 and I'1 were of type 2. Composition A' used the KH ternary feldspar and XB plagioclase. Its bulk composition is close to that of G. A tie line drawn between the fields of AF and PF products in A'1 does not pass through the bulk composition. The bulk composition of the reactant assemblage lies somewhere along the tie line connecting AF and PF (labeled A'1) and is richer in Ab than the starting composition. The same is true for experiment I'1. Therefore, we have not demonstrated complete exchange equilibrium in these type 2 700 °C experiments. We assumed from our time-series experiments on composition G that 115 days would be sufficient at 700 °C to react the starting minerals, but it was not. However, there was significant reaction in compositions A and I, and the fields of reactant AF and PF define a smooth miscibility gap. It is possible that early in the reaction of these phases some of the plagioclase starting material was mantled and removed from reaction with the rest of the starting material, and the coexisting feldspars may represent local exchange equilibrium established among the unmantled starting materials available for reaction.

The experiments at 700 °C, 2 kbar produced many 5 to 15 μm crystals of ternary feldspar and reaction overgrowths on unreacted grains of starting mineral grains (Fig. 2A). The smaller crystals of plagioclase and alkali feldspar in Figure 2A are homogeneous, the darker gray large plagioclase grains are compositionally zoned, and the larger alkali-feldspar crystals contain homogeneous overgrowth rims and patchy cores that contain unhomogenized albite lamellae.

Experiments at 650–700 °C, 2–3 kbar. Experiments A4 and G5 contained binary plagioclase and alkali feldspar

(HM + LH + XB) starting materials (Fig. 3). As in the example above, tie lines connecting the AF and PF reaction products pass through the bulk compositions. Therefore, reaction was nearly complete, and these runs demonstrate type 1 equilibrium. The coexisting AF and PF in G10-2 and G10-9 were produced by reaction with melt. The AF and PF fields produced in experiments using A and G are similar, and tie lines are parallel, indicating that comparable products were produced through reaction mechanisms involving fluid and melt.

Experiments at 800 °C, 2 kbar. Initially, experiments at 800 °C, 2 kbar were conducted for 31 days (experiment G3). The crystalline products are small, homogeneous crystals surrounded by melt and larger crystals that developed reaction overgrowth rims. The compositional variation in the small crystals and in the overgrowth rims was identical, and there was no relation between composition of rim and location between overgrown core and reaction rim. In addition, a significant amount of Ab-Or-rich melt was generated. In the case of G3, the fields of AF and PF and the Ab-Or-rich melt define a triangle that contains the bulk composition. Therefore, nearly complete reaction occurred after 31 days.

A BSE SEM image of one of the experiments at 800 °C (Fig. 2B) shows reaction textures typical of those that develop when melt is present. The light gray alkali feldspars contain euhedral overgrowth rims and unreacted cores of feldspar (HM) that contain vestiges of unhomogenized albite lamellae. The Na-rich plagioclase (LH) is reacted and embayed in outline, and the Ca-rich plagioclase (XB) contains a more Na-rich overgrowth.

Experiments K1 and L1 used HM + LH + XB as starting materials and were carried out at 800 °C for 14 days. Melt was present in these experiments, but the tie line connecting fields of product AF and PF lie on the Ab-rich side of the bulk compositions. Experiments P1 (San + LH + XB) and Q1 (San + SA + XB) used different sets of three binary-feldspar starting materials, and reactants coexisted with fluid. Sanidine was used as the Or-rich AF to see if the structural state of the starting minerals influenced the final compositions (Type 3). Tie lines connecting the fields of product AF and PF also pass to the Ab-rich side of the bulk compositions (Fig. 5). In all of the experiments at 800 °C, 2 kbar the XB starting material is overgrown by reaction rims. All of these experiments underwent significant reaction and produced AF and PF fields that outline a smooth miscibility gap. The tie lines connecting fields of AF and PF for each experiment are generally parallel. For these reasons we retained these experiments and used them in the following thermodynamic analysis. Of these experiments at 800 °C, G3 most likely contains products that achieved exchange equilibrium, whereas the other four experiments are problematic.

Experiments at 880–900 °C, 1 kbar. At these conditions experiments L3, P2, M1, and O1 underwent nearly complete reaction of starting materials. Experiments L3 and P2 were of approximately the same bulk composition but

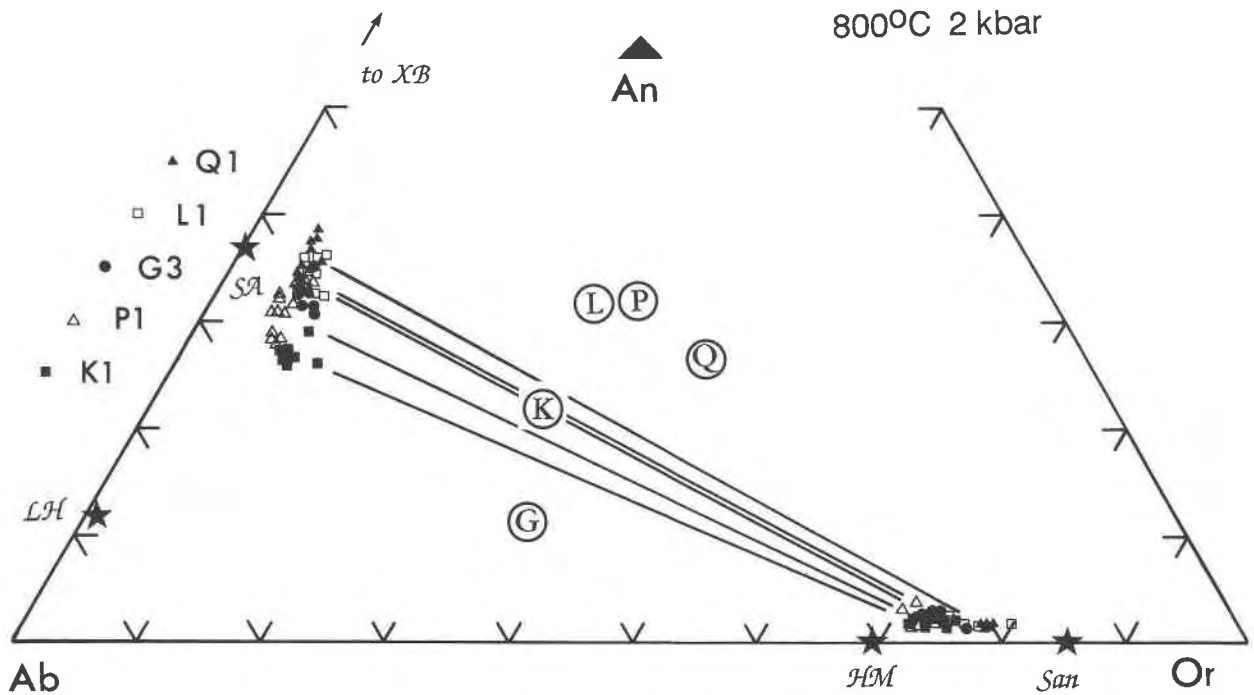


Fig. 5. Compositional variation in product AF and PF produced in the experiments at 800 °C, 2 kbar. See Tables 1 and 3 for compositions and starting materials. Bulk compositions are shown as open circles enclosing letters.

used different three-crystal binary starting assemblages. Experiment L3 used HM + LH + XB and experiment P2 used San + LH + XB. Products and reaction paths are shown in Figures 6 and 7 along with the bulk compositions and the crystalline starting material compositions. Experiments L3 and P2 both melted, and their bulk compositions lie inside a triangle defined by the fields of AF and PF and an Ab-Or-rich melt ($\approx \text{Ab}_{42}\text{Or}_{52}\text{An}_6$). Both experiments have similar tie-line orientations for the fields of AF and PF and similar amounts of Or in PF and An in AF reactant products. Therefore, experiments L3 and P2 demonstrate type 1 equilibrium. In experiment M1 the bulk composition lies barely within the triangle defined by the tie line connecting fields of AF and PF and an Ab-Or-rich melt ($\approx \text{Ab}_{56}\text{Or}_{40}\text{An}_4$). In experiment KL1 the triangle defined by the coexisting AF, PF, and melt ($\approx \text{Ab}_{56}\text{Or}_{40}\text{An}_4$) lies on the Ab-rich side of the bulk composition. The An-rich plagioclase in this starting material was isolated from reaction by rims of reactant AF and PF. Because experiment KL1 underwent extensive reaction, the results are reported here and used in the modeling. Experiment O1 started with a mix of ternary feldspar KxLH and XB and represents a type 2 reaction. A tie line drawn between the fields of coexisting AF and PF products from this experiment passes through the bulk composition.

Experiments at 600 °C, 2 kbar. The experiments conducted for 189 days at 600 °C, 2 kbar did not contain measurable reaction rims.

Summary of experimental results

Our experiments produced consistent product compositions by approaching the same reaction product AF and PF pairs from different bulk starting compositions. The experiments that used two feldspars as starting compositions (Aⁿ1, Iⁿ1, and O1) converge on the ternary miscibility gap from within the ternary and provide half brackets on the rotation of tie lines. The three mineral starting compositions show an approach to metastable or stable equilibrium, when the final compositional fields for AF and PF are tightly clustered and the bulk composition of the starting material lies on a tie line connecting the AF and PF fields or within a 3-phase triangle melt-AF-PF. These criteria are met or nearly met for the following experiments: G2, A4, G5, E2, G3, L3, P2, and M1. The other three mineral experiments are problematic. We did not attempt to evaluate the Al-Si order in our products. Since we used natural starting materials in these experiments, we assume that the overgrowth reaction rims are relatively well-ordered, but we do not know if this order has approached equilibrium. Starting materials that used natural feldspars with disordered and ordered Al-Si produced similar AF and PF compositions, so there does not appear to be any noticeable effect on Ca-K-Na exchange from variations in Al-Si order of the crystalline starting materials. Although we did not characterize Al-Si order, we can compare our experiments to others where Al-Si ordering kinetics have been studied. Carpenter (1986) de-

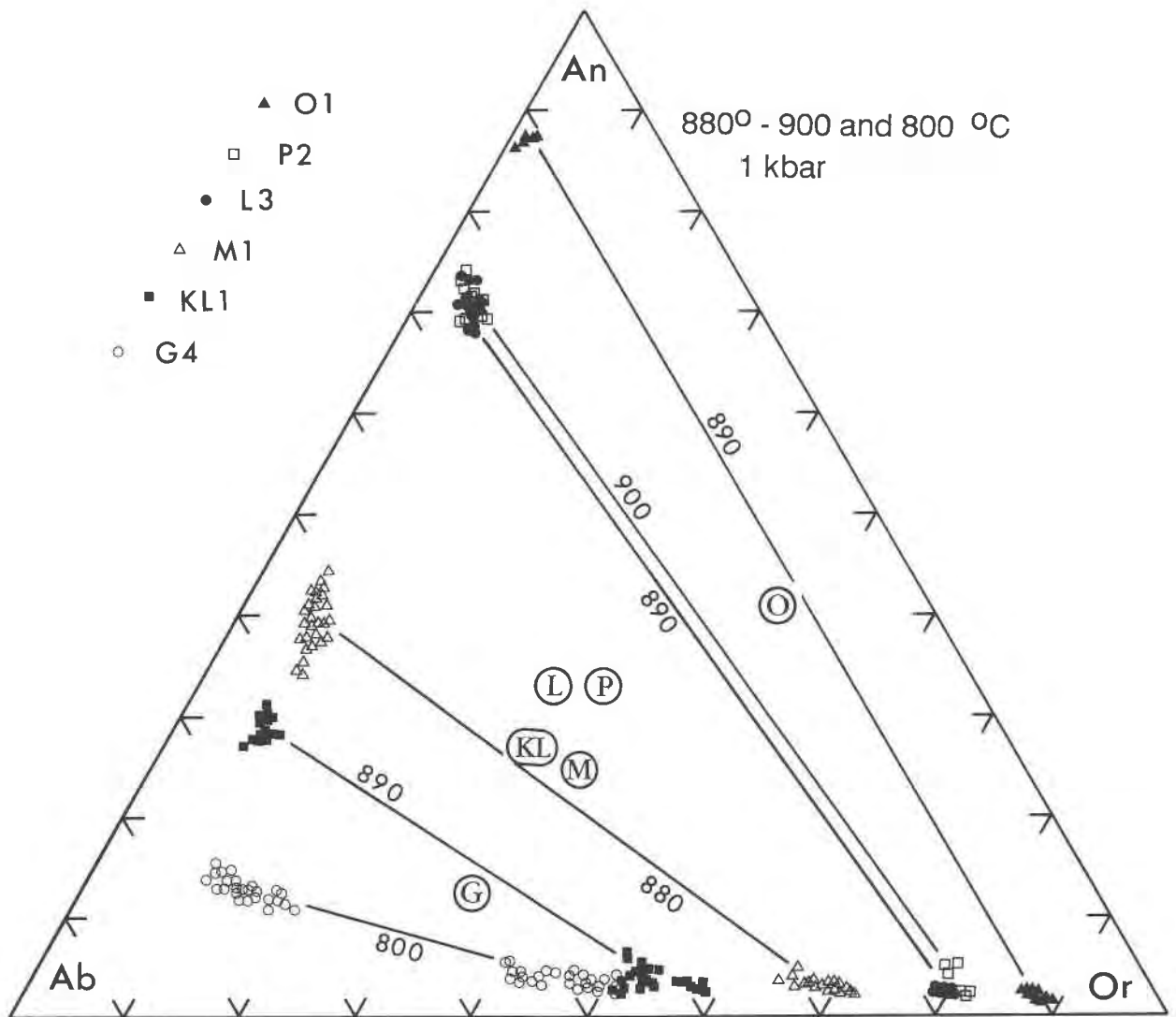


Fig. 6. Compositional variation in AF and PF produced in 1-kbar experiments. See Tables 1 and 3 for starting materials and reactant compositions. With the exception of experiment G4 (800 °C), experiments were carried out over the temperature interval 880–900 °C. Bulk compositions are shown as open circles enclosing letters.

terminated Al-Si ordering kinetics in plagioclase under hydrothermal conditions and found that very little change in ordering occurs at 700 °C after one year, and that times of at least three months are required at 800–850 °C. Since our experiment times at comparable temperatures were shorter than Carpenter's, it is most probable that our product feldspars are of high structural state.

ACTIVITY MODEL FOR TERNARY FELDSPAR COMPONENTS

We have followed the method outlined by Ghiorso (1984) and revised by Fuhrman and Lindsley (1988), with some further modifications to their approach. At equilibrium the chemical potentials of Ab, An, and Or in co-

existing plagioclase (PF) and alkali (AF) feldspar are equal.

$$\mu_{Ab}^{PF} = \mu_{Ab}^{AF} \quad (1)$$

$$\mu_{An}^{PF} = \mu_{An}^{AF} \quad (2)$$

$$\mu_{Or}^{PF} = \mu_{Or}^{AF} \quad (3)$$

For each phase the equilibrium conditions may be expressed in terms of a standard-state free-energy term for each component and a free energy of mixing.

$$\mu_{Ab}^{PF} = \mu_{Ab}^{0PF} + RT \ln a_{Ab}^{PF}$$

and

$$\mu_{Ab}^{AF} = \mu_{Ab}^{0AF} + RT \ln a_{Ab}^{AF}$$

As in all previous treatments of ternary feldspar equilibria, we assume that the PF and AF phases are part of a continuous solution, are tied to the same standard-state free energies for each component, and that the μ^0 's are equal for each component in each phase. Therefore, the conditions for equilibrium reduce to

$$a_{Ab}^{PF} = a_{Ab}^{AF} \quad (4)$$

$$a_{An}^{PF} = a_{An}^{AF} \quad (5)$$

$$a_{Or}^{PF} = a_{Or}^{AF} \quad (6)$$

Configurational entropy

Ghiorso (1984) expanded the configurational entropy expression developed by Kerrick and Darken (1975) to account for the ideal part of the free energy of solution that would be expected if mixing took place in the feldspar solution so that Al-Si ordering followed the Al-avoidance principle. Newton et al. (1980) also found that such an expression for the ideal part of the solution was required in order to reconcile their measurements of the excess enthalpy of solution for high structural-state plagioclase with the cation-exchange experiments of Orville (1972). In developing a model for feldspar-liquid equilibria, Nekvasil and Burnham (1987) found that an Al-avoidance model for plagioclase could not be reconciled with their experimental data and adopted an ideal single-site model for the ideal part of the free energy of mixing. Lindsley and Nekvasil (1989) refined the Fuhrman and Lindsley (1988) ternary feldspar model, also adopting a single-site model for the ideal part of the mixing term. In our initial efforts to develop a thermodynamic model for our ternary feldspar data, we attempted to use the Al-avoidance expression but found that it always produced a large dispersion in the temperatures estimated by the three equilibrium conditions. Our models using the Al-avoidance expression predict the temperature of our experiments to within ± 30 °C using the Or equilibrium constraint (Equilibrium 1) over the temperature range spanned by our data (650 to 900 °C). Temperatures predicted using the Ab and An equilibrium constraint varied as a function of temperature. At 700 °C, temperatures predicted from the An equilibrium constraint were always 50 to 100 °C too high. At 800 °C, temperatures predicted by our model from the Ab condition of Equilibrium 1 were systematically 100 °C low. At 900 °C the temperatures from Ab and An were widely divergent. When an ideal mixing model was adopted, and when we used our experimental data to predict the excess free energy for the Ab-An binary (discussed below), our ability to recover measured temperature from our experimental data improved.

Activity expressions for ternary feldspars

For the excess free energy of mixing for ternary feldspar we adopted a ternary Margules expression that includes asymmetric terms for each binary and a ternary interaction term (Wohl, 1953; Andersen and Lindsley, 1981).

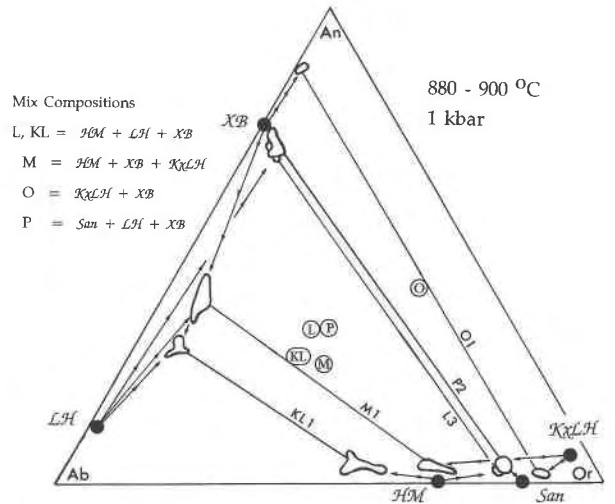


Fig. 7. Products, starting minerals, and bulk compositions for selected experiments at 880–900 °C, 1 kbar. Solid dots and script initials show starting minerals. Bulk compositions are shown by circles enclosing letters. Product compositions lie within the elliptical areas, and AF and PF fields from each experiment are connected by a tie line showing experiment number. Arrows point from starting mineral compositions to reactant products.

Assuming an ideal single-site model for the configurational entropy of mixing ($-TS_{\text{config}}$) and a ternary asymmetric Margules expression for the excess free energy of mixing (G_{ex}), the expressions for the activity coefficients in Equations 4, 5, and 6 are:

$$a_{Ab} = X_{Ab} \cdot \exp\left\{ \left(W_{OrAb} [2X_{Ab}X_{Or}(1 - X_{Ab}) + X_{Or}X_{An}(1/2 - X_{Ab})] \right. \right. \\ + W_{AbOr} [X_{Ab}^2(1 - 2X_{Ab}) + X_{Or}X_{An}(1/2 - X_{Ab})] \\ + W_{AbAn} [X_{Ab}^2(1 - 2X_{Ab}) + X_{Or}X_{An}(1/2 - X_{Ab})] \\ + W_{AnAb} [2X_{An}X_{Ab}(1 - X_{Ab}) + X_{Or}X_{An}(1/2 - X_{Ab})] \\ + W_{OrAn} [X_{Or}X_{An}(1/2 - X_{Ab} - 2X_{An})] \\ + W_{AnOr} [X_{Or}X_{An}(1/2 - X_{Ab} - 2X_{Or})] \\ \left. \left. + W_{OrAbAn} [X_{Or}X_{An}(1 - 2X_{Ab})] \right) / RT \right\} \quad (7)$$

$$a_{An} = X_{An} \cdot \exp\left\{ \left(W_{OrAb} [X_{Ab}X_{Or}(1/2 - X_{An} - 2X_{Ab})] \right. \right. \\ + W_{AbOr} [X_{Ab}X_{Or}(1/2 - X_{An} - 2X_{Or})] \\ + W_{AbAn} [2X_{Ab}X_{An}(1 - X_{An}) + X_{Ab}X_{Or}(1/2 - X_{An})] \\ + W_{AnAb} [X_{Ab}^2(1 - 2X_{An}) + X_{Ab}X_{Or}(1/2 - X_{An})] \\ + W_{OrAn} [2X_{Or}X_{An}(1 - X_{An}) + X_{Ab}X_{Or}(1/2 - X_{An})] \\ + W_{AnOr} [X_{Or}^2(1 - 2X_{An}) + X_{Ab}X_{Or}(1/2 - X_{An})] \\ \left. \left. + W_{OrAbAn} [X_{Or}X_{Ab}(1 - 2X_{An})] \right) / RT \right\} \quad (8)$$

TABLE 4. Excess free-energy terms for ternary feldspars

	Furhman and Lindsley (1988)			This study		
	W_H	W_S	W_V	W_H	W_S	W_V
W_{AbOr}	18810	10.3	0.394	18810	10.3	0.4602
W_{OrAb}	27320	10.3	0.394	27320	10.3	0.3264
W_{AbAn}	28226			7924 (525)		
W_{AnAb}	8471			0.0		
W_{OrAn}	47396			40317 (460)		
W_{AnOr}	52468		-0.120	38974 (292)		-0.1037
W_{AbOrAn}	8700		-1.094	12545 (965)		-1.095

Note: $W_G = W_H - TW_S + PW_V$. Units are joules, kelvins, and bars. Ab-Or excess terms: W_H and W_S terms are from Haselton et al. (1983). W_V terms are from Hovis (1988). Parenthesized units are 1σ errors on parameters determined by least squares fits to the experimental data. W_V terms for An-Or and Ab-Or-An are from Lindsley and Nekvasil (1989).

$$\begin{aligned}
 a_{Or} = X_{Or} \cdot \exp\{ & (W_{OrAb}[X_{Ab}^2(1 - 2X_{Or}) \\
 & + X_{Ab}X_{An}(1/2 - X_{Or})] \\
 & + W_{AbOr}[2X_{Ab}X_{Or}(1 - X_{Or}) \\
 & + X_{Ab}X_{An}(1/2 - X_{Or})] \\
 & + W_{AbAn}[X_{Ab}X_{An}(1/2 - X_{Or} - 2X_{An})] \\
 & + W_{AnAb}[X_{Ab}X_{An}(1/2 - X_{Or} - 2X_{Ab})] \\
 & + W_{OrAn}[X_{An}^2(1 - 2X_{Or}) \\
 & + X_{Ab}X_{An}(1/2 - X_{Or})] \\
 & + W_{AnOr}[2X_{Or}X_{An}(1 - X_{Or}) \\
 & + X_{Ab}X_{An}(1/2 - X_{Or})] \\
 & + W_{OrAbAn}[X_{An}X_{Ab}(1 - 2X_{Or})]/RT \} \quad (9)
 \end{aligned}$$

These equations are identical to those of Fuhrman and Lindsley (1988), except that the configurational entropy term assumes ideal mixing on a single site. Equations 7, 8 and 9 for each phase are substituted into the conditions of Equilibrium 4, 5, and 6. The resulting expression can then be simplified by collecting terms and used to solve for unknown excess parameters (W_{ij}). Alternatively, the expressions can be used to solve for temperature. Following Ghiorso (1984) and Fuhrman and Lindsley (1988), we first rearrange the substituted expression so that the unknown terms are on one side of the equation and a constant term consisting of known parameters is on the other. We have 60 equations derived from the 20 experiments that we may use to solve for the unknown excess parameters (W_{ij}) with the method of least squares.

Earlier calibrations of the excess free energy (Ghiorso, 1984; Green and Udansky, 1986; Fuhrman and Lindsley, 1988) used published Margules parameters for the Or-Ab and Ab-An joins and calculated values for the Or-An binary. Fuhrman and Lindsley (1988) summarize the parameter choices of those models that were based on Seck's (1971a, 1971b) experimental data. In our initial attempts to model our own experimental data, we also used published values for the Or-Ab and Ab-An joins, the Al-

avoidance model for the configurational entropy, and, following the method of Fuhrman and Lindsley (1988), solved for the Or-An binary excess terms. We used the method of least squares, adjusted the compositions of our experiments within the limits of compositional variability to optimize the fit, and obtained parameter estimates. Through this technique we were able to generate excess parameters and errors on the parameters that were similar to those of Fuhrman and Lindsley (1988). However, when we used these parameter estimates and the adjusted values of the phase compositions to estimate temperatures, those temperature estimates diverged widely for the Ab and An equilibria. A similar result was obtained when we used the estimates by Lindsley and Nekvasil (1989) of the Ab-Or and Ab-An binaries and the single site configurational entropy terms. Again, the best model using the adjusted compositions predicted widely divergent temperatures for the Ab and An equilibrium conditions.

In the model reported in Table 4, we used published values for W_{AbOr} and W_{OrAb} and solved for the remaining five parameters W_{AbAn} , W_{AnAb} , W_{OrAn} , W_{AnOr} , and W_{OrAbAn} . The excess volume (W_V) terms for the Or-An binary and the ternary W_V from Lindsley and Nekvasil (1989) were fixed. Of the five parameters, the W_{AnAb} term determined by least squares was always small (100–300 J), and the error was larger than the term. Accordingly, this term was set to zero. We solved for the asymmetric Margules parameters using the method of least squares, adjusting compositions of our experimental products within the limits of compositional variability to optimize the fit and obtain parameter estimates with the smallest errors (Table 4). The adjusted compositions of our experimental products are in Table 5.

The W_{OrAn} , W_{AnOr} and W_{OrAbAn} terms estimated using our model are similar in magnitude to those of Fuhrman and Lindsley (1988) and Lindsley and Nekvasil (1989). Our model for the Ab-An join contains only one excess term. The activity coefficients calculated for Ab on the An-Ab binary over the range 700–900 °C give $\gamma_{Ab} \approx 1$ from An_0 to An_{50} and $\gamma_{Ab} > 1$ from An_{50} to An_{100} . The activity coefficients calculated for An give $\gamma_{An} \approx 1.1$ –1.2 over the binary. These values of γ_{Ab} and γ_{An} calculated by our model are similar to those estimated by Carpenter and Ferry (1984), who also modeled the configurational entropy as single-site mixing, and expressed deviations from ideality with an excess entropy of ordering (ΔS_{ord}).

In our model the total free energy of mixing in the Ab-An binary [composed of the G_{ex} and configurational entropy ($-TS_{config}$) terms] is similar to that obtained by Newton et al. (1980) from their fit of enthalpy of solution data in the binary Ab-An system. The measurements of excess enthalpy of solution by Newton et al. (1980) are in Figure 8 along with the Newton et al. model, and the model derived from our ternary feldspar experiments for Ab-An. The models are very similar and provide equally good fits to the enthalpy of solution data of Newton et al. (1980). The reason that the two models are so similar has to do with the relative contributions from the

TABLE 5. Adjusted compositions of coexisting AF and PF used to generate the ternary-feldspar solution model

Experiment	Alkali feldspar			Plagioclase feldspar			T°C	P bars
	Ab	Or	An	Ab	Or	An		
L3	0.170	0.799	0.031	0.255	0.032	0.713	890	1000
KL1	0.420	0.535	0.045	0.642	0.097	0.261	890	1000
M1	0.300	0.665	0.035	0.545	0.070	0.385	880	1000
O1	0.093	0.880	0.027	0.120	0.023	0.857	890	1000
P2	0.155	0.815	0.030	0.240	0.035	0.725	900	1000
G4	0.483	0.492	0.025	0.732	0.153	0.115	800	1000
K1	0.282	0.700	0.018	0.635	0.095	0.270	800	2000
L1	0.243	0.740	0.017	0.590	0.065	0.345	800	2000
G3	0.257	0.724	0.019	0.595	0.062	0.343	800	2000
P1	0.270	0.712	0.018	0.622	0.066	0.312	800	2000
Q1	0.214	0.770	0.016	0.570	0.065	0.365	800	2000
G2	0.276	0.715	0.009	0.732	0.053	0.215	700	2000
E2	0.331	0.660	0.009	0.772	0.078	0.149	700	2000
I'1	0.423	0.568	0.009	0.740	0.205	0.055	700	2000
A'1	0.408	0.580	0.012	0.797	0.084	0.119	700	2000
G10-2	0.251	0.740	0.009	0.720	0.058	0.222	700	2000
G5	0.333	0.657	0.010	0.773	0.072	0.155	700	3000
A4	0.331	0.658	0.011	0.763	0.072	0.165	700	3000
G10-7	0.255	0.736	0.009	0.720	0.050	0.230	675	2000
G10-9	0.232	0.763	0.005	0.772	0.060	0.168	650	3000

Note: Temperatures calculated in Figure 9 use these compositions as input.

$-TS_{\text{config}}$ and G_{ex} terms in each model. In the Newton et al. (1980) model, the Kerrick and Darken (1975) approximation to $-TS_{\text{config}}$ adds a large negative contribution that is compensated by a larger positive G_{ex} term. In our single-site model the $-TS_{\text{config}}$ term is smaller and the contribution from G_{ex} is smaller. The resulting free energy of mixing is about the same in the binary Ab-An system. The activity model for Ab-An proposed here is probably not adequate to account for the ordering that becomes important at temperatures below 700 °C (Salje et al., 1985), but it is the best simple model of plagioclase activity over the temperature range covered by the experiments.

Using the model in Table 4 we were able to recover better estimates of the temperatures of our experiments than those obtained by fitting our data using the models of Fuhrman and Lindsley (1988) or Lindsley and Nekvasil (1989). When the three conditions of equilibrium were used to predict temperature (from the adjusted compositions used to obtain the best fit), temperature recovery was very good. Figure 9 shows the values of temperature predicted by the model. In most cases the errors are within ± 20 °C of the experimental temperature. However, there are still a few experiments at 800 °C and 700 °C for which the temperatures estimated from the Ab equilibria are low by 30 to 60 °C. As a further comparison we used the two-feldspar thermometer program of Fuhrman and Lindsley (1988), appropriately substituted with our thermodynamic model, and calculated temperatures for the experiments of Seck (1971a) and Johannes (1979). Seck's 17 experiments at 750 °C, 1 kbar gave an average temperature of 773 °C, which is 23 °C higher than the reported experimental temperature. Seck's 13 experiments at 825 °C, 1 kbar gave an average temperature of 852 °C, which is 27 °C higher than the experimental tem-

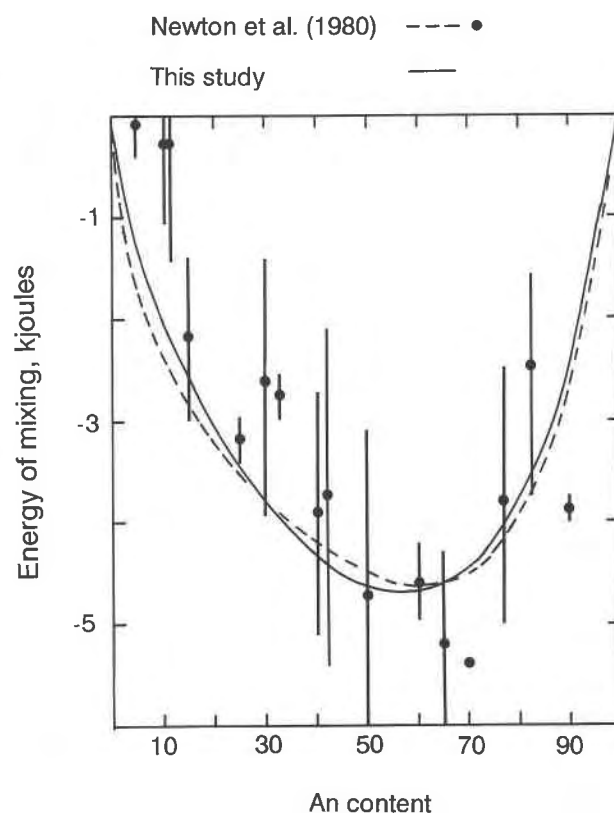


Fig. 8. Enthalpy of mixing from Newton et al. (1980) for the Ab-An binary at 970 °K. Solid dots show measurements of Newton et al. with 2 σ error bars. Dashed line is G_{soln} calculated using the Newton et al. model, which includes an Al-avoidance term in the ideal-mixing term and a G_{ex} term. Solid line is G_{soln} calculated assuming an ideal mixing on a single site and a G_{ex} term.

TABLE 6. Comparison of calculated temperatures for igneous and metamorphic ternary-feldspar pairs

	P (kb)	Feldspar (PF then AF)			Fuhrman and Lindsley (1988)			This study		
		Ab	Or	An	T _{Ab}	T _{Or}	T _{An}	T _{Ab}	T _{Or}	T _{An}
Experiments										
Johannes (1979)	1	0.540	0.060	0.400				780	778	790
800 °C		0.240	0.750	0.010						
800 °C	1	0.510	0.060	0.430				730	765	745
		0.200	0.790	0.010						
Volcanic rocks										
Carmichael (1965)	1	0.654	0.073	0.273	849	821	832	868	863	862
Trachyte		0.379	0.603	0.018						
Ewart (1965)	1	0.632	0.041	0.326	807	756	776	813	782	796
Ignimbrite [750 °C]*		0.319	0.653	0.028						
Hildreth (1979)		0.798	0.061	0.141	676	676	671	687	679	680
Bishop Tuff [720 °C]	1	0.362	0.630	0.008						
[780 °C]	1	0.702	0.076	0.222	770	772	779	769	770	770
		0.337	0.650	0.013						
Baldrige et al. (1981)										
Leucite	0.001	0.253	0.029	0.718	909	892	902	947	949	952
basanite		0.168	0.791	0.041						
Phonolite	0.001	0.477	0.072	0.451	905	868	903	952	951	949
-tephrite		0.293	0.675	0.003						
Plutonic rocks										
Fuhrman and Lindsley (1988)	3	0.544	0.286	0.170	984	984	989	1049	1055	1046
Monzonite		0.417	0.484	0.100						
Monzosyenite	3	0.553	0.278	0.181	884	885	921	930	1006	931
Parsons and Brown (1983)	1	0.342	0.612	0.047						
Syenogabbro	1	0.520	0.260	0.220	932	932	970	998	1052	1004
		0.330	0.610	0.060						
Metamorphic rocks										
Bohlen and Essene (1977)										
BM-15	8	0.743	0.014	0.242	707	612	708	698	618	685
		0.235	0.751	0.014						
IN-11	8	0.785	0.017	0.193	764	604	750	763	615	746
		0.348	0.639	0.006						
MM-2	8	0.762	0.030	0.205	723	665	725	728	680	807
		0.256	0.700	0.036						
SR-31	8	0.713	0.010	0.273	763	598	766	786	616	720
		0.314	0.638	0.031						
SC-2	8	0.722	0.008	0.270	675	582	626	672	603	668
		0.196	0.800	0.004						
XY-9	8	0.796	0.014	0.183	770	583	704	783	602	741
		0.196	0.800	0.004						
XY-12	8	0.808	0.013	0.178	778	590	779	775	594	720
		0.385	0.586	0.026						

* Fe-Ti-oxide temperatures shown in [].

perature, and the 11 experiments at 900 °C and 1 kbar gave an average temperature of 886 °C, which is 14 °C lower than the experimental temperature. The two assemblages at 800 °C, 1 kbar reported by Johannes gave average temperature estimates of 746 and 783 °C, which are 54 and 17 °C below the temperature of the experiment (Table 6). The temperature recovery for Johannes' experiments is similar to that obtained from our own experimental data and would be expected, since Johannes demonstrated exchange equilibrium for his experiments at 800 °C.

APPLICATIONS TO THERMOMETRY-BAROMETRY

Feldspars from volcanic and plutonic rocks

Fuhrman and Lindsley (1988) compared their feldspar thermometer with the feldspar thermometers of Ghiorso (1984), Green and Udansky (1986), and Haselton et al. (1983) and concluded that their thermometer represented

a significant improvement over the previous thermometers. Along with their thermodynamic model, Fuhrman and Lindsley (1988) developed a program for estimating temperature by adjusting feldspar compositions within analytical uncertainty and using all three conditions of equilibrium. We have followed the same method and used their feldspar thermometer program (M_{THERM3}) modified to incorporate our thermodynamic model. Table 6 shows a comparison of temperatures calculated for feldspar pairs from volcanic and plutonic igneous rocks.

For volcanic rocks our temperature estimates are slightly higher than those of Fuhrman and Lindsley (1988), and the differences in temperature among the three equilibria are equal to or smaller than the differences in estimates from the model of Fuhrman and Lindsley (1988). Rhyolites containing two feldspars are a common rock type likely to retain high-temperature feldspar compositions by quenching on eruption. Fe-Ti-oxide geothermometry is the method of choice for estimating pre-eruptive tem-

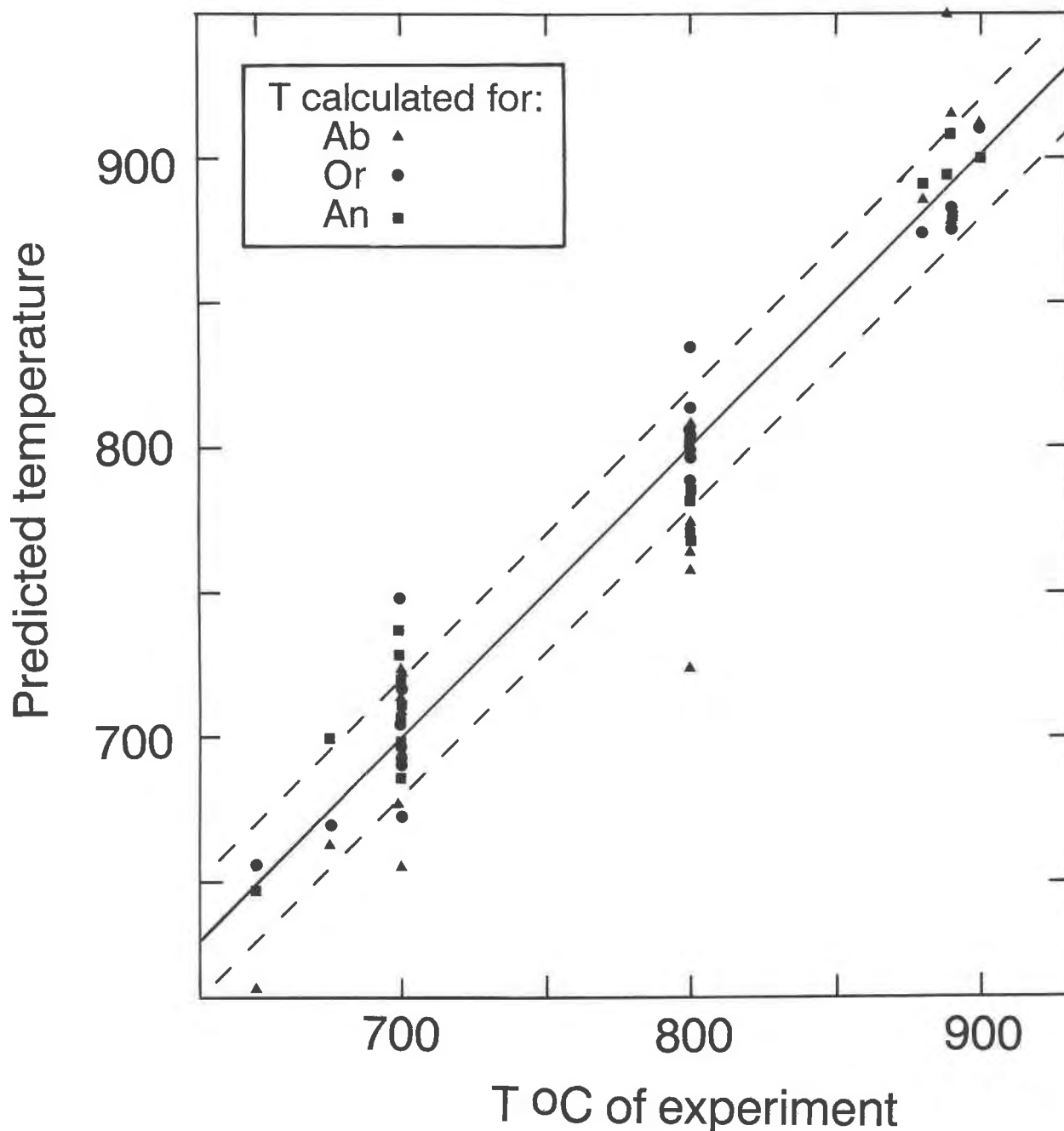
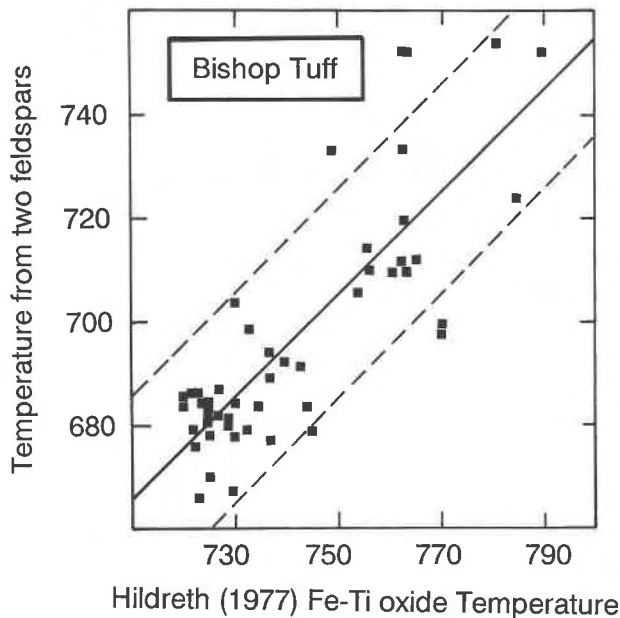


Fig. 9. Temperatures calculated for experiments using the parameters presented in Table 4. Horizontal axis shows temperature of experiment, and vertical axis shows calculated temperature. Each of the three conditions of equilibrium was used to predict temperature. Ab = triangles, Or = circles and An = squares. Dashed lines are $\pm 20^\circ\text{C}$ from the predicted $T = \text{experimental } T$ line.

temperatures in rhyolites. Table 6 shows two examples of Fe-Ti-oxide and two-feldspar temperatures, using data from Ewart (1965) and Hildreth (1979). In many rhyolites two Fe-Ti oxides are not present, or the oxide compositions have been altered by low-temperature oxidation. In these instances an accurate two-feldspar thermometer would be extremely useful for estimating temperature. We assess

this application of two-feldspar thermometry by applying it to the data presented by Hildreth (1977) on the thermally and chemically zoned Bishop Tuff. Hildreth (1977) reports 56 coexisting Fe-Ti-oxide and AF-PF feldspar pairs and temperature estimates from Fe-Ti-oxide thermometry. Fe-Ti-oxide and two-feldspar temperature estimates are compared in Figure 10 and show an encour-



Hildreth (1977) Fe-Ti oxide Temperature

Fig. 10. Temperatures calculated for 56 coexisting AF-PF feldspar pairs from the Bishop Tuff using *M_{THERM3}* (Fuhrman and Lindsley, 1988) and the thermodynamic model presented in this paper compared with estimates of temperature from Fe-Ti-oxide thermometry (Hildreth, 1977). Solid line is a regression fit to the data, and dashed lines show ± 20 °C deviation. Two feldspar temperatures are the average of temperatures estimated from the three conditions of equilibrium.

aging consistency. The two-feldspar temperature estimates are averages for the three equilibria, and the 56 pairs show an average difference of 8 °C for calculated temperatures. The two-feldspar temperatures are systematically lower than the Fe-Ti-oxide temperatures, but the feldspar temperatures record the same temperature zonation found with the Fe-Ti-oxide temperatures. A regression line with ± 20 °C limits contains 50 of the 56 samples.

Comparing our thermometer to that of Fuhrman and Lindsley (1988) for strongly ternary feldspars from plutonic rocks, our model predicts temperatures that are higher. In the case of the Laramie anorthosite complex (Table 6, monzonite) our two-feldspar temperatures are higher than the temperature range estimated using two-pyroxene thermometry (980–1020 °C). Our feldspar temperature for the Klokken syenogabbro also lies at the high end of the temperature range estimated by Parsons and Brown (1983).

Feldspars from metamorphic rocks

Table 6 shows temperatures calculated for coexisting feldspars from Adirondack granulite-facies rocks. Our results are similar to those of Fuhrman and Lindsley (1988) for these samples. We find that the temperature estimate from the Ab and An equilibrium conditions are similar and that the temperature calculated from the Or equilibrium is much lower, often by more than 100 °C. As Fuhr-

man and Lindsley (1988) suggest, changes in composition caused by exsolution or alkali exchange may have modified these feldspar pairs after they equilibrated at some peak metamorphic temperature.

ACKNOWLEDGMENTS

Steve Recca expertly maintained the JEOL Superprobe 733 and offered advice and assistance with the analytical work. Tom Sisson provided the analytical data on Himalayan granite G10. The authors thank Carl Francis and the Harvard Mineralogical Museum for providing starting materials for this study. We thank W. L. Brown, M. A. Carpenter, T. C. Juster, R. J. Kinzler, D. H. Lindsley, S. I. Recca, and T. W. Sisson for providing thoughtful and stimulating reviews. This research was supported by NSF grants EAR-8517327 and EAR-8721097.

REFERENCES CITED

- Albee, A.L., and Ray, L. (1970) Correction factors for electron microprobe microanalysis of silicates, oxides, carbonates, phosphates and sulphates. *Analytical Chemistry*, 42, 1408–1414.
- Andersen, D.J., and Lindsley, D.H. (1981) A valid Margules formulation for an asymmetric ternary solution: Revision of the olivine-ilmenite thermometer, with applications. *Geochimica et Cosmochimica Acta*, 45, 847–853.
- Baldrige, W.S., Carmichael, I.S.E., and Albee, A.L. (1981) Crystallization paths of leucite-bearing lavas: Examples from Italy. *Contributions to Mineralogy and Petrology*, 76, 321–335.
- Barth, T.F.W. (1951) The feldspar geologic thermometers. *Neues Jahrbuch für Mineralogie Abhandlungen*, 82, 143–154.
- Bence, A.E., and Albee, A.L. (1968) Empirical correction factors for electron microanalysis of silicates and oxides. *Journal of Geology*, 76, 382–403.
- Bohlen, S.R., and Essene, E.J. (1977) Feldspar and oxide thermometry of granulites in the Adirondack Highlands. *Contributions to Mineralogy and Petrology*, 62, 153–169.
- Brown, W.L., and Parsons, I. (1981) Towards a more practical two-feldspar geothermometer. *Contributions to Mineralogy and Petrology*, 76, 369–377.
- Carmichael, I.S.E. (1965) Trachytes and their feldspar phenocrysts. *Mineralogical Magazine*, 34, 107–125.
- Carpenter, M.A. (1986) Experimental delineation of the “e”-I1 and “e”-C1 transformations in intermediate plagioclase feldspars. *Physics of Chemistry and Minerals*, 13, 119–139.
- Carpenter, M.A., and Ferry, J.M. (1984) Constraints on the thermodynamic mixing properties of plagioclase feldspars. *Contributions to Mineralogy and Petrology*, 87, 138–148.
- Carter, J.L. (1970) Mineralogy and chemistry of the earth’s upper mantle based on the partial fusion–partial crystallization model. *Geological Society of America Bulletin*, 81, 2021–2034.
- Ewart, A. (1965) Mineralogy and petrogenesis of the Whakamaru ignimbrite in the Maraetai area of the Taupo volcanic zone, New Zealand. *New Zealand Journal of Geology and Geophysics*, 8, 611–677.
- Fuhrman, M.L., and Lindsley, D.H. (1988) Ternary feldspar modeling and thermometry. *American Mineralogist*, 73, 201–215.
- Ghiorso, M.S. (1984) Activity/composition relations in the ternary feldspars. *Contributions to Mineralogy and Petrology*, 87, 282–296.
- Green, N.L., and Udansky, S.I. (1986) Ternary-feldspar mixing relations and feldspar thermobarometry. *American Mineralogist*, 71, 1100–1108.
- Grice, J.D., and Gault, R.A. (1983) Lapis lazuli from Lake Harbor, Baffin Island, Canada. *Rocks and Minerals*, 58, 13–19.
- Harlow, G.E., and Brown, G.E., Jr. (1980) Low albite: An X-ray and neutron diffraction study. *American Mineralogist*, 65, 986–995.
- Haselton, H.T., Jr., Hovis, G.L., Hemingway, B.S., and Robie, R.A. (1983) Calorimetric investigation of the excess entropy of mixing in analbite-sanidine solid solutions: Lack of evidence for Na, K short-range order and implications for two-feldspar thermometry. *American Mineralogist*, 68, 398–413.
- Hildreth, W. (1977) The magma chamber of the Bishop Tuff: Gradients

- in temperature, pressure and composition, 328 p. Ph.D. thesis, University of California, Berkeley, California.
- (1979) The Bishop tuff: Evidence for the origin of compositional zonation in silicic magma chambers. Geological Society of America Special Paper 180, 45–75.
- Hovis, G.L. (1986) Behavior of alkali feldspars: Crystallographic properties and characterization of composition and Al-Si distribution. *American Mineralogist*, 71, 869–890.
- (1988) Enthalpies and volumes related to K-Na mixing and Al/Si order/disorder in alkali feldspars. *Journal of Petrology*, 29, 731–763.
- Iiyama, J.T. (1966) Contribution à l'étude des équilibre sub-solidus du système ternaire orthose-albite-anorthite à l'aide des réactions d'échange d'ions Na-K au contact d'une solution hydrothermale. *Bulletin du Société Minéralogie et Cristallographie, Français*, 89, 442–454.
- Johannes, W. (1979) Ternary feldspars: Kinetics and possible equilibria at 800 °C. *Contributions to Mineralogy and Petrology*, 68, 221–230.
- Kerrick, D.M., and Darken, L.S. (1975) Statistical thermodynamic models for ideal oxide and silicate solid solutions, with applications to plagioclase. *Geochimica et Cosmochimica Acta*, 39, 1431–1442.
- Lindsley, D.H., and Nekvasil, H. (1989) A ternary feldspar model for all reasons (abs.). *EOS*, 70, 506.
- McConnell, J.D.C. (1974) Analysis of the time-temperature-transformation behavior of the plagioclase feldspars. In W.S. MacKenzie and J. Zussman, Eds., *The feldspars*, p. 460–490. Manchester University Press, Manchester, United Kingdom.
- Nekvasil, H., and Burnham, C.W. (1987) The calculated individual effects of pressure and water content on phase equilibria in the granite system. In B.O. Mysen, Ed., *Magmatic processes: Physicochemical principles*, p. 433–445, The Geochemical Society, University Park, PA.
- Newton, R.C., Charlu, T.V., and Kleppa, O.J. (1980) Thermochemistry of high structural state plagioclases. *Geochimica et Cosmochimica Acta*, 44, 933–941.
- Orville, P.M. (1967) Unit-cell parameters of the microcline—low albite and the sanidine—high albite solid solution series. *American Mineralogist*, 52, 55–86.
- (1972) Plagioclase cation exchange equilibria with aqueous chloride solution: Results at 700 °C and 2000 bars in the presence of quartz. *American Journal of Science*, 272, 234–272.
- Parsons, I., and Brown, W.L. (1983) A TEM and microprobe study of a two-perthite alkali gabbro: Implications for the ternary feldspar system. *Contributions to Mineralogy and Petrology*, 82, 1–12.
- Powell, M., and Powell, R. (1977) Plagioclase-alkali feldspar geothermometry revisited. *Mineralogical Magazine*, 41, 253–256.
- Price, J.G. (1985) Ideal site-mixing in solid solutions with applications to two-feldspar geothermometry. *American Mineralogist*, 70, 696–701.
- Salje, E., Kuscholke, B., and Kroll, H. (1985) Thermodynamics of sodium feldspar: II. Experimental results and numerical calculations. *Physics and Chemistry of Minerals*, 12, 99–107.
- Seck, H.A. (1971a) Koexistierende alkalifeldspate und plagioklase im system $\text{NaAlSi}_3\text{O}_8$ - KAlSi_3O_8 - $\text{CaAl}_2\text{Si}_2\text{O}_8$ - H_2O bei temperaturen von 650 °C bis 900 °C. *Neues Jahrbuch für Mineralogie Abhandlungen*, 115, 315–342.
- (1971b) Die einfluß des drucks auf die zusammensetzung koexistierende alkalifeldspate und plagioklase im system $\text{NaAlSi}_3\text{O}_8$ - KAlSi_3O_8 - $\text{CaAl}_2\text{Si}_2\text{O}_8$ - H_2O . *Contributions to Mineralogy and Petrology*, 31, 67–86.
- Stormer, J.C., Jr. (1975) A practical two-feldspar geothermometer. *American Mineralogist*, 60, 667–674.
- Thompson, J.B., Jr., Waldbaum, D.R., and Hovis, G.L. (1974) Thermodynamic properties related to ordering in end member alkali feldspars. In W.S. MacKenzie and J. Zussman, Eds., *The feldspars*, p. 218–248. Manchester University Press, Manchester.
- Tuttle, O.F. (1949) Two pressure vessels for silicate-water studies. *Geological Society of America Bulletin*, 60, 1727–1729.
- Whitney, J.A., and Stormer, J.C., Jr. (1977) The distribution of $\text{NaAlSi}_3\text{O}_8$ between coexisting microcline and plagioclase and its effect on geothermometric calculations. *American Mineralogist*, 62, 687–691.
- Wohl, K. (1953) Thermodynamic evaluation of binary and ternary liquid systems. *Chemical Engineering Progress*, 49, 218–219.

MANUSCRIPT RECEIVED MAY 9, 1989

MANUSCRIPT ACCEPTED FEBRUARY 5, 1990